Article

Applied Spectroscopy

Applied Spectroscopy
2016, Vol. 70(8) 1328–1338

DOI: 10.1177/0003702816654063
asp.sagepub.com

SAGE

Structural Evolution of Silica Gel and Silsesquioxane Using Thermal Curing

Nan Hu[1], YuanQiao Rao[2], Shengtong Sun[3], Lei Hou[3], Peiyi Wu[3], Shaojuan Fan[4], and Bangjiao Ye[4]

Abstract

The curing of coatings of two types of siloxane containing materials, silica gel and silsesquioxane, at a modest temperature (<280°C) was studied with in situ heating Fourier transform infrared spectroscopy (FT-IR) in combination with perturbation correlation moving window (PCMW) and two-dimensional correlation spectroscopy (2D-COS) analyses. The result revealed detailed structural evolution of these two different gels. When the silica gel was heated, $(Si–O)_6$ rings appeared from the random Si–O–Si network formed after sol gel reaction, followed by condensation of silanol groups. Upon further heating, the existing $(Si–O)_4$ rings were broken down and converted into $(Si–O)_6$ structures, and finally isolated silanols appeared. The transition from $(Si–O)_4$ rings to $(Si–O)_6$ rings was observed by IR and further confirmed with positron annihilation lifetime spectroscopy (PALS). In comparison, during the curing of hybrid silsesquioxane, the condensation of silanols happens immediately upon heating without the rearrangement of Si–O–Si network. Afterwards, the fraction of $(Si–O)_6$ ring structure increased. $(Si–O)_4$ structures exhibited higher stability in hybrid silsesquioxanes. In addition, the amount of silanols in silsesquioxane continued to reduce without the generation of isolated silanol in the end. The different curing behavior of silsesquioxanes from silica gel originates from the organic groups in silsesquioxanes, which lowers the cross-linking density and reduces the rigidity of siloxane network.

Keywords

Silica gel, Silsesquioxane, infra-red (IR) spectroscopy, perturbation correlation moving window (PCMW), two-dimensional correlation spectroscopy, positron annihilation lifetime spectroscopy (PALS)

Date received: 18 August 2015; accepted: 30 November 2015

Introduction

The generation of inorganic or organic/inorganic hybrid functional materials at a modest temperature has been of long-standing interest. Sol-gel chemistry is one facile method towards this goal. Silica gel and silsesquioxane (SSQ) are two silicon-containing materials that can be made through sol-gel chemistry. After forming and casting of the pre-polymer sols, they are usually thermally cured, typically below 300°C for low temperature curing, to be transformed into useful products.[1] While silica gel has a repeat unit of SiO_2, silsesquioxane has a repeat unit of $RSiO_{1.5}$ (R represent organic groups). Silsesquioxane can be synthesized by the co-hydrolysis and condensation of tetra alkoxy silanes and a variety of organic substituted trialkoxy silanes. The structure and properties of the silsesquioxane product can be greatly affected by the organic composition. Since the 1950s, silica gel and silsesquioxane have been explored for different applications, such as glass resin/siloxane resins for heat-resistant coatings, release coatings, automobile exhausts, engine components, and others.[2] Over the last two decades, silica gel and silsesquioxane have been applied in lithography, sensing, and opto-materials and extensively studied as low-K dielectrics.[3–6] In the 1990s, polyhedral oligomeric silsesquioxane (POSS) was commercialized and stirred focused exploration of this unique cage molecule.[7]

This paper concerns the silica gel and silsesquioxane that do not have complete cage-like structures and may contain

[1]The Dow Chemical Company, Shanghai, China
[2]The Dow Chemical Company, Freeport, TX, USA
[3]State Key Laboratory of Molecular Engineering of Polymers, Department of Macromolecular Science, and Laboratory of Advanced Materials, Fudan University, Shanghai, China
[4]State Key Laboratory of Particle Detection and Electronics, University of Science and Technology of China, Hefei, China

Corresponding author:
Nan Hu, 2030 Dow Center, Midland, MI 48674, USA.
Email: harlyhn@sohu.com

residual reactive groups, especially silanols or silicon alkoxides. The film-coating properties of silica gel and silsesquioxane, such as their optical, dielectric, tensile, and thermal properties, are significantly altered by two critical structural components: the siloxane network structure and the types of end groups, in particular silanols. The condensation reactions among different species are different and lead to different final structures and properties.

The formation of a silica gel and silsesquioxane coating involves the following steps. First, prepare precursor (prepolymer) sol from the hydrolysis and condensation of tetra alkoxy silane and organic substituted trialkoxy silane. Second, coat the precursor sol on to a substrate and dry the solvent. And lastly, thermally cur the coating to form desired morphology/structure. The cross-linking structure of silica gel and silsesquioxane is constructed via the condensation of silanol groups during the drying process and further advanced by curing afterwards. Both chemical composition and curing condition will affect the final structure. Therefore, understanding the structural evolution upon the curing process is of great importance.[8]

Infrared (IR) spectroscopy is sensitive to morphology and conformational changes by reflecting subtle information at the molecular level.[9,10] There have been many literature articles on IR spectra of sol-gel synthesized silicon polymer, which will be further discussed in a later section.[11–17] Nevertheless, there is a general lacking of in depth understanding of the kinetics of structural change so as to guide the structural optimization towards desired properties. In this paper, the thermal cross-linking process of silica gel and silsesquioxane was detected by in situ heating Fourier transform infrared spectroscopy spectroscopy (FT-IR). We utilized perturbation correlation moving window (PCMW) in combination with two-dimensional correlation spectroscopy (2D-COS) technologies to derive structural changes in siloxane network and silanols.

Positron annihilation lifetime spectroscopy (PALS) is a sensitive tool to nanoscale void and free volume of material. In the past decades, structures of amorphous materials have been intensively studied by this technology. By combination with a secondary electron in the material, the injected positron will generate a positron–electron pair, positronium (Ps). Annihilation behavior of formed triplet positronium (o–Ps) provides the structural information of the nanovoid/free volume in material, such as size, concentration, etc. Hence, PALS has been well accepted as a probe of nanovoid and free volume nowadays.[18,19] Here, we used this technology to further examine the siloxane structure.

With the combination of the PCMW, 2D-COS, and PALS, both the silanol condensation and Si–O–Si skeleton formation during thermal curing were studied on a silica gel and a silsesquioxane. By comparing the results of both materials, the impact of organic groups on the microstructure is revealed.

Experimental Section

Synthesis of Silica and Silsesquioxane Sols

Raw Materials. Tetraethyl orthosilicate (TEOS) and methyltrimethoxysilane (MTMS) were purchased from Sigma-Aldrich. All the other reagents, including hydrochloric acid and propylene glycol monomethyl ether acetate (PGMEA), were obtained from Sinopharm Chemical Reagent Co. All samples were used as received.

Tetraethyl Orthosilicate Homopolymer (Homo-TEOS). Tetraethyl orthosilicate (20.83 g, 0.10 mol) was added into PGMEA (13.34 g). Mechanical stirring was applied to the solution. Dilute aqueous HCl (1.00 g, 0.100 M) was mixed with 7.21 g H_2O. Then the solution was added into the PGMEA solution drop wise within 30 min. After that, the solution was stirred at room temperature for another 30 min. Then it was heated to 60°C for 2 h and subsequently to 100°C for 20 min to remove the distillate. A transparent solution of homo-TEOS was obtained. The weight average molecular weight (Mw) of homo-TEOS is 2200 with a polydispersity index of 1.69, determined by gel permeation chromatography (GPC).

Tetraethyl Orthosilicate–Trimethoxymethylsilane Co-Polymer (TM (30–70)). Silsesquioxane solution was prepared with a similar procedure except the heating condition was changed to 70°C for 2 h followed by 100°C for 30 min. TM (30–70) was prepared with a mixture of monomers containing 30 mol% tetraethyl orthosilicate and 70 mol% trimethoxymethylsilane.[3–6] The weight average molecular weight (M_w) of TM (30–70) is 2600 with a polydispersity index of 1.90, determined by GPC.

Sample Preparation and Characterization

Gel Permeation Chromatography. Gel permeation chromatography was carried out in THF (flow rate: 1 mL/min) at 35°C with a Waters 515 HPLC pump equipped with a Waters 2410 refractive index detector and three Waters Styragel HR columns (103, 104, and 105 Å pore sizes) in series. Monodisperse polystyrene standards were used for calibration.

Fourier Transform Infrared Spectroscopy. The sample solution was cast on a KBr plate and dried under vacuum at room temperature for 2 days. Infrared spectra were recorded in transmission mode with Thermo Scientific™ NICOLET 6700. To ensure the full removal of PGMEA solvent, the absence of IR peak of carbonyl band (at around 1700 cm^{-1}) from PGMEA was checked, as illustrated in Figures S1 and S2, available online in the Supplemental Material. A hot plate was installed as an accessory for the in situ heating. Samples were heated from 40°C to 280°C at the rate of about 2°C/min, and IR spectra were recorded manually with an interval of 5°C.

Positron Annihilation Lifetime Spectroscopy. The positron lifetime experiments were carried out with a fast–fast coincidence system (ORTEC Co.) with a time resolution of about 230 ps in full width at half-maximum. The positron source for the lifetime measurements was 30 μCi ^{22}NaCl, which was dropped on Kapton membrane. The source was sandwiched between two identical samples under study and the total count was two million. Melt routine was utilized for the data analysis.[20]

Infrared Investigation Methods

Perturbation Correlation Moving Window. Fourier transform infrared spectra collected at an increment of 5°C during heating were used to perform PCMW analysis. Primary data processing was carried out with the method Morita provided[21] and further correlation calculation was performed using the software 2D Shige, Ver. 1.3 (Shigeaki Morita, Kwansei-Gakuin University, Japan, 2004–2005). The final contour maps were plotted by Origin program, ver. 8.0, with warm colors (red and yellow) defined as positive intensities and cool colors (blue) as negative ones. An appropriate window size ($2m + 1 = 11$) was chosen to generate PCMW spectra with good quality.

Two-Dimensional Correlation Spectroscopy. Fourier transform infrared spectra used for PCMW analysis were also used to perform 2D-COS. Two-dimensional correlation analysis was carried out using the same software 2D Shige ver. 1.3 (Shigeaki Morita, Kwansei-Gakuin University, Japan, 2004–2005), and was further plotted into the contour maps by Origin program ver. 8.0. In the contour maps, warm colors (red and yellow) are defined as positive intensities, while cool colors (blue) are defined as negative ones.

Results and Discussion

Introduction of Conventional Infrared Analysis on Sol-gel Silicon Polymer

There have been many literature articles on IR spectra of sol-gel synthesized silicon polymers.[11–17] In general, stretching bands of SiO–H at 3800–3000 cm^{-1} and stretching bands of Si–O–Si bond at 1200–1000 cm^{-1} have been studied the most. Infrared bands in these two regions are the combination of several sub-peaks arising from various microstructures (Scheme 1). There is still debate on the assignment and explanation of these sub-peaks. Table I shows some tentative assignments of several IR peaks. Specifically, stretching peaks of silanols are affected by hydrogen bond association. Peaks of isolated silanols exhibit the highest wavenumber 3750–3680 cm^{-1}, while peaks of mono-hydrogen-bonded (3600–3400 cm^{-1}) and poly-hydrogen-bonded silanols (around 3200 cm^{-1}) locate at lower wavenumber regions. On the other hand, the structures of the Si–O–Si network are more complicated. They exist in ring structures formed by a couple of Si–O tetrahedrons. Based on quantum calculation, there should be a broad distribution in the number of Si–O tetrahedron per ring.[11] Relatively, the $(Si–O)_4$ and $(Si–O)_6$ rings are more predominating and thus have been better studied among all the Si–O rings. The $(Si–O)_4$ ring forms several structures such as open cage, closed cage, and ladder. The IR absorption peak at around 1150 cm^{-1} arises from $(Si–O)_4$ ring asymmetric stretch vibration.[12] Existence of this peak indicates the presence of a highly symmetrical molecular structure such as closed cage. The peak at around 1050 cm^{-1} is attributed to the $(Si–O)_4$ ring symmetric stretch vibration mainly from asymmetric random network structures such as open cage and short ladder.[12] Indeed, the IR spectrum of a commercial octamethyl POSS, which is a well-defined and

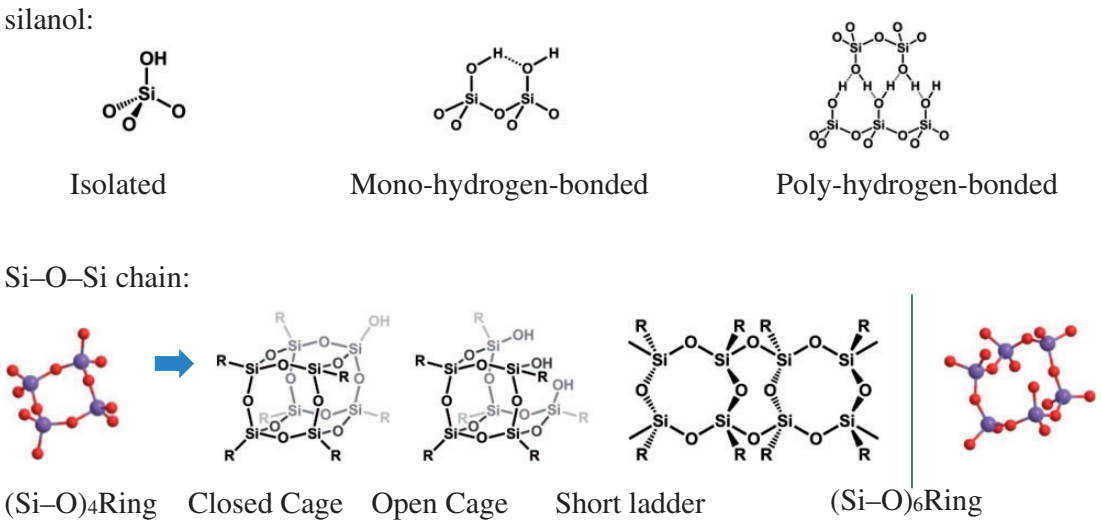

Scheme 1. Microstructures of silanols and Si–O–Si chain in sol-gel synthesized polysiloxane.

Table 1. Tentative peak assignment in a Sol-Gel SSQ Films based on the literature.[9,12,15–17]

IR band assignment	Structural origin	Spectral peak (cm^{-1})
Stretching of SiO–H	Isolated silanol	3680–3750
	SiO–H bonded to Si–O–Si	3676
	Mono-hydrogen-bonded	3400–3600
	Poly-hydrogen-bonded silanols	3200
Si–O–Si asymmetric stretching from siloxane microstructure	Asymmetric $(Si–O)^4$ ring stretch vibration (closed cage)	1150
	Symmetric $(Si–O)^4$ ring stretch vibration (branched random network, open cage, short ladder)	1050
	$(Si–O)^6$ ring stretch vibration	1036

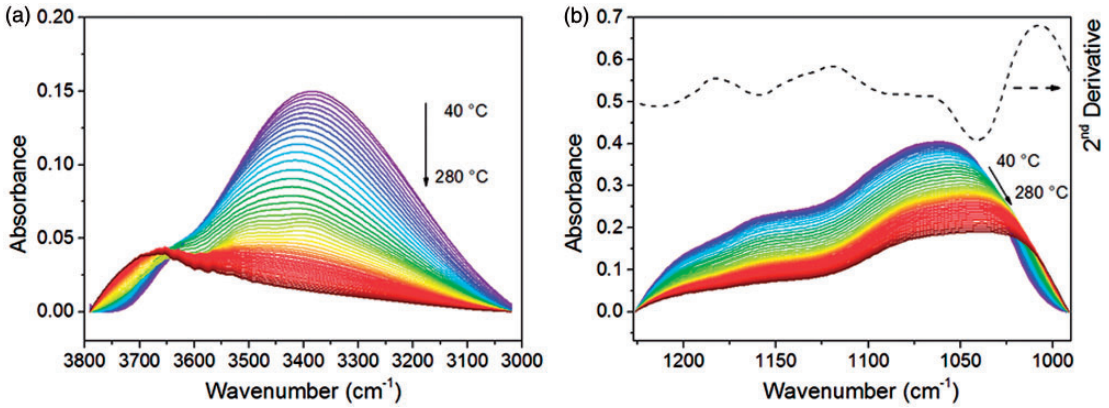

Figure 1. In situ heating IR spectra of home-TEOS from 40°C to 280°C with 5°C of intervals. (a) Infrared band of silanol stretching. (b) Infrared band of Si–O–Si stretching. The dashed line represents the second derivate spectrum of home-TEOS heated at 40°C.

highly symmetric T8 cage, has one strong, narrow Si–O stretching band at 1107 cm^{-1} instead of two broader Si–O stretching bands.[13] It was also reported that compared to the thermally grown silicon oxide, the sharp peak near 1050 cm^{-1} is narrower for the silica gel film, indicating some mobility in the silica gel sample.[14] Compared with the $(Si–O)_4$ ring, the $(Si–O)_6$ ring with the characteristic peak at 1036 cm^{-1} is a more organized and thermodynamically favorable network structure similar to the basic unit of the SiO_2 crystal.

Homo-TEOS

Conventional Infrared Analysis. To monitor the cross-linking process, an in situ heating IR test was performed on homo-TEOS from 40°C to 280°C with intervals of 5°C. Infrared spectra of silanol stretching and Si–O–Si stretching were exclusively examined as shown in Figure 1. With an increase of temperature, the intensity of the O–H stretching peak of the silanol group decreased dramatically due to silanol condensation. In addition, the peak position shifted to a higher wavenumber region, which means the relative content of isolated silanol groups to hydrogen-bonded silanols kept increasing upon heating. This is likely because the associated (hydrogen-bonded) silanol groups can condense more easily with each other compared to the isolated ones. Meanwhile, the shape of the Si–O–Si stretching peak also changed gradually upon heating. According to Figure 1b, the shape of Si–O–Si stretching peak (1250 ~ 1000 cm^{-1}) is a broad asymmetric band comprising several peaks. This region is of great interest as it comprises microstructure information. In general, the band in the region of 1200–1000 cm^{-1} shifted to lower wavenumber upon heating.

Perturbation Correlation Moving Window. Perturbation Correlation Moving Window is a newly developed technique, whose basic principles date back to the conventional moving window proposed by Thomas.[22] In 2006 Morita improved this technique to much wider applicability through introducing a perturbation variable into the correlation equation.[21] Together with its original ability in determining transition points as the conventional moving window does, PCMW can additionally monitor complicated spectral variations along the perturbation direction.

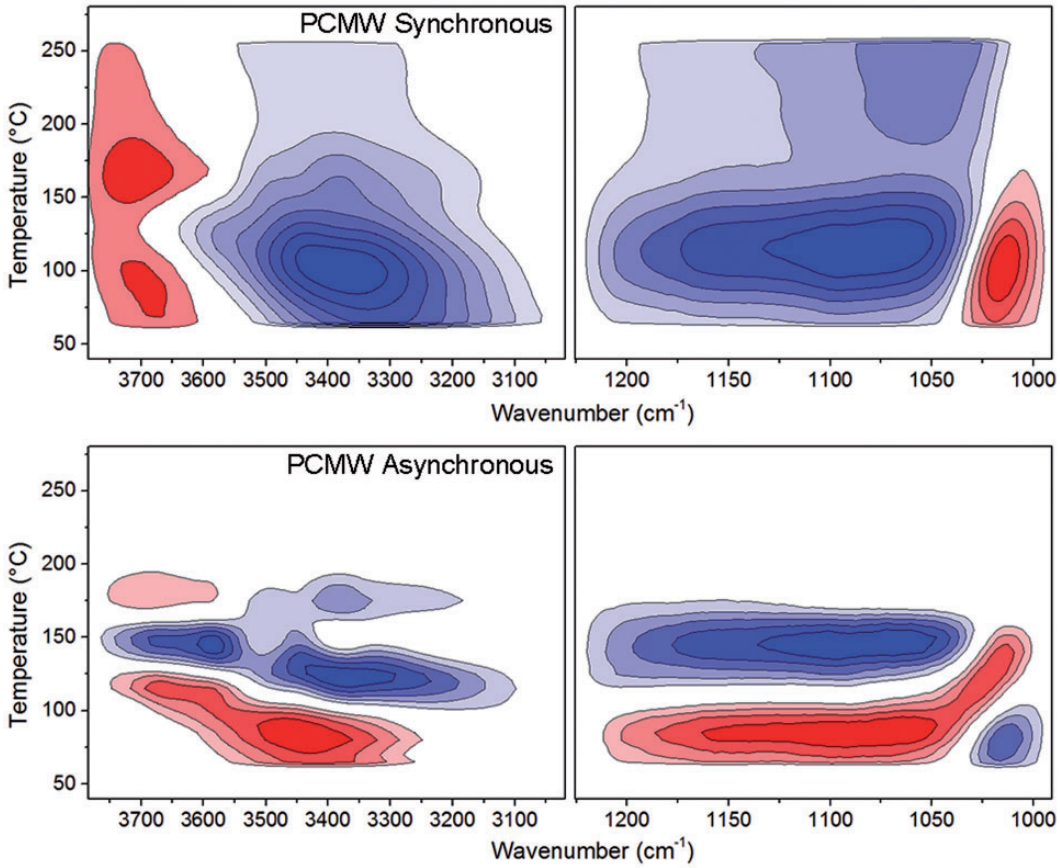

Figure 2. Perturbation correlation moving window (PCMW) analysis of in situ heating IR spectra of homo-TEOS. The warm color (red) means a positive change in intensity, while the cold color (blue) represents a negative change in intensity.

With this technique, a synchronous spectrum and an asynchronous spectrum can be generated. The rules of PCMW can be summarized as follows: a positive synchronous correlation represents spectral intensity increase, while a negative one represents decrease; a positive asynchronous correlation represents a convex spectral intensity variation while a negative one represents a concave variation.[13,14] Therefore in synchronous spectrum, the peak position indicates the transition point. The transition could be reaction, glass transition, phase separation, etc. In an asynchronous spectrum, the peaks indicate the onset and endpoints of the transition.

Figure 2 represents the PCMW synchronous and asynchronous spectra generated from the temperature resolved spectra. In the synchronous spectrum of the silanol stretching region, the spectral intensity in 3550–3100 cm^{-1} kept decreasing with an increase of temperature. Reversely, the band at 3760–3600 cm^{-1} was growing upon heating, though the intensity increase was rather weak. These observations suggest that hydrogen-bonded silanols were condensed during heating. As a result, the residual silanols were structurally isolated from one another and cannot condense without further breaking or rearrangement of Si–O–Si network. The newly formed isolated silanols should be the residual of condensation between hydrogen-bonded silanols. In terms of the Si–O–Si stretching region, different trends also existed. With an increase of temperature, the intensity of 1200–1040 cm^{-1} dropped while the intensity of 1040–1000 cm^{-1} increased. As summarized above, the peaks of $(Si–O)_4$ rings concentrates at former region and the peak of $(Si–O)_6$ ring locates at the latter one. The result implies that the cross-linked siloxane assumes more fraction of $(Si–O)_6$ rings and some $(Si–O)_4$ rings were transformed into $(Si–O)_6$ rings during the curing process. This phenomenon will be further discussed below.

Combining the synchronous and asynchronous spectra, we summarize the effect of temperature on the changes of various IR bands in Table 2. Note that the 3760–3600 cm^{-1} band exhibited two weak peaks corresponding to two maximum increasing rates in the synchronous spectrum. The onset temperature of the first one did not appear in the asynchronous spectrum because it was lower than the starting temperature of PCMW spectra (60°C). Only the second peak at 165°C was included in Table 2. Interestingly, the four IR bands in Table 2 show various transition temperature ranges. The decreasing of

Table 2. Change of characteristic spectra peaks affected by curing temperature in homo-TEOS polymers.

Changed IR bands	Direction of intensity change	Onset temperature (°C)	Peak temperature (°C)	End temperature (°C)
3760–3600 cm^{-1}, isolated silanol	Increase	145	165	180
3500–3100 cm^{-1}, hydrogen-bonded silanol	Decrease	80	100	125
1200–1040 cm^{-1}, Si–O–Si in the $(Si–O)_4$ ring	Decrease	85	115	145
1040–1000 cm^{-1}, Si–O–Si in the $(Si–O)_6$ ring	Increase	80	100	125

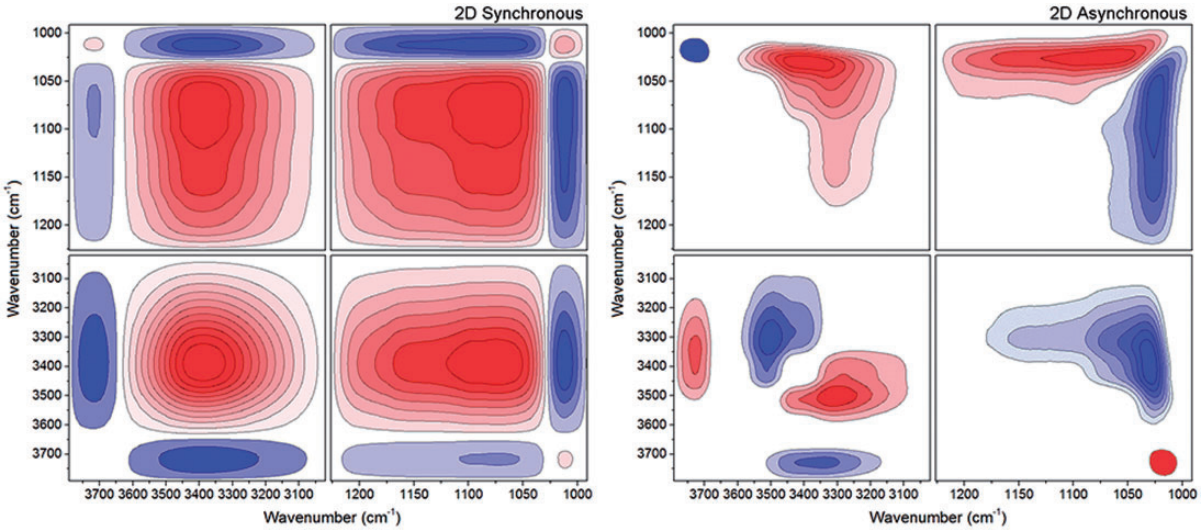

Figure 3. Two-dimensional synchronous and asynchronous spectra analysis of homo-TEOS generated from all spectra between 60°C and 200°C during heating. Herein, the warm color (red) represents the positive correlation of peaks, while the cold color (blue) represents the negative correlation of peaks.

the hydrogen-bonded silanol peak and increasing of the $(Si–O)_6$ ring peak happened first, which was followed by the decreasing of the $(Si–O)_4$ ring peak. Increasing of the isolated silanol peak was the last step of the spectral evolution. This result indicates that the structural transition upon thermal curing is a consecutive process with changes of various microstructures in sequence. Using 2D-COS technology, we have resolved the types of the microstructure and the precise transition process, which will be discussed next. Overall the formation of a cross-linked Si–O–Si network mainly happened in the temperature range of 80–145°C. This observation suggests that a minimum temperature of 145°C is required to achieve a fairly high cross-linking density when using silica gel. In the region of 145–280°C there was still intensity change in the synchronous spectrum, which indicated condensation between residual silanols still existed with an increase of temperature. This phenomenon is expected because completing the silanol condensation requires thermal treatment at above 600°C for the sol gel synthesized silica.[8]

Two-Dimensional Correlation Spectroscopy. In the previous section, we confirmed that the evolution of the IR spectra is the result of different changes in the structure happening consecutively. In order to understand the structural transition of homo-TEOS further, 2D-COS was performed in this paper. Two-dimensional correlation spectroscopy is a mathematical method whose basic principles were first proposed by Noda in 1986.[15] Up to the present time, 2D-COS has been widely used to study spectral variations of different chemical species under various external perturbations. Due to the different responses of different species to external variables, additional useful information about molecular motions or conformational changes can be extracted which cannot be obtained from conventional one-dimensional spectra. Similar to the PCMW described above, a synchronous spectrum and an asynchronous 2D spectrum of homo-TEOS are shown in Figure 3. The judging rule can be summarized as Noda's rule- that is, if the cross-peaks (ν_1, ν_2, and assume $\nu_1 > \nu_2$) in synchronous and asynchronous spectra have the same signs, the change at ν_1 may occur prior to that of ν_2, and vice versa.[23]

Figure 3 shows the synchronous and asynchronous spectra from 2D-COS analysis. The key benefit of the asynchronous spectrum is that it can significantly enhance the resolution of IR spectrum. According to the self-correlated asynchronous spectrum, the cross-peaks of silanol and Si–O–Si network structures were resolved, which related to spectral changes during heating. According to assignments in Table 1, there are five peaks in the silanol stretching region: 3728 cm^{-1} (isolated silanols), 3500 cm^{-1} (mono-hydrogen-bonded silanols), 3404 cm^{-1}, 3342 cm^{-1}, and 3309 cm^{-1} (poly-hydrogen-bonded silanols).[15] In terms of Si–O–Si stretching, peaks at 1070 cm^{-1} (open cage and short ladder of $(Si–O)_4$ ring), 1030 cm^{-1}, and 1018 cm^{-1} ($(Si–O)_6$ ring) were distinguished.[9,12,16,17] To the best of our knowledge, detailed assignment of $(Si–O)_6$ IR peaks have not been well studied yet. We tend to believe that peaks at 1030 cm^{-1} and 1018 cm^{-1} should be assigned to the $(Si–O)_6$ ring with various conformations. Synchronous spectrum clearly showed that the intensities of 3728 cm^{-1}, 1030 cm^{-1}, and 1018 cm^{-1} increased while intensities of other peaks decreased. Besides, there are two more hidden peaks locating at around 1210 and 1160 cm^{-1} in the conventional IR spectrum (Figure 1b), which become more apparent in the second derivate spectrum of homo-TEOS heated at 40°C. These two peaks, however, were not distinguished in 2D-COS. This is probably evidence that the corresponding groups were not affected in heating process. Their assignments are not clear.

Using Noda's rules, we were able to deduce the response sequence of the eight peaks: 1018 cm^{-1} → 3309 cm^{-1} → 3342 cm^{-1} → 3404 cm^{-1} → 3500 cm^{-1} → 1070 cm^{-1} → 3728 cm^{-1} → 1030 cm^{-1}. This sequence explained the detailed structural transition process of homo-TEOS pre-polymers during heating. Interestingly, the rearrangement of Si–O–Si chain to form a $(Si–O)_6$ ring indicated by 1018 cm^{-1} peak took place ahead of condensation of silanols. The siloxane network probably formed in pre-polymer synthesis and subsequent drying is highly stressed and, when provided with energy upon heating, rearranges into more stable $(Si–O)_6$ rings and also offers accessibility to different silanol groups to condense. After that, the silanol condensation started with the sequence of 3309 cm^{-1} → 3342 cm^{-1} → 3404 cm^{-1} → 3500 cm^{-1}. This reaction sequence is consistent with the decrease of the hydrogen-bonding strength of silanols, which means hydrogen bonding between silanols can facilitate the condensation. The collapse of the open cage and short ladders of $(Si–O)_4$ ring at 1070 cm^{-1} followed the condensation. It can be explained that these stressed $(Si–O)_4$ structures would transform into a highly cross-linking network with $(Si–O)_6$ units. Moreover, the development of isolated silanol occurred as the residual product of condensation. Last in sequence, the $(Si–O)_6$ structure with IR peak of 1030 cm^{-1} formed as the results of silanol condensation as well as rearrangement of Si–O–Si chain. At this time, the Si–O–Si network has been highly cross-linked. Thus, the formed $(Si–O)_6$ ring was frozen to a distorted conformation and thus exhibited a higher wavenumber response.

It is well-known that the glass transition temperature of the Si–O–Si skeleton is around 600°C, below which the frozen Si–O–Si structure totally reflects the result of sol-gel condensation. If the transition of $(Si–O)_4$ rings to $(Si–O)_6$ rings detected by IR does happen, the free volume of Si–O–Si skeleton should increase due to the larger void size of the $(Si–O)_6$ ring. Positron annihilation lifetime spectrum, an irreplaceable probe at angstrom level, has been extensively used to detect the atomic void and free volume in materials.[19,24,25] To monitor the free volume change of Si–O–Si skeleton, PALS was used to measure the change of free volume. Generally, the positrons injected in the material exhibit three lifetimes, τ_1, τ_2, and τ_3. Only the species that have a lifetime that is longer than 0.5 ns, typically τ_3, is related to the size of free volume. Assuming the free volume is spherical, the τ_3 lifetime could be transformed into the average radius of free volume using a semi-empirical method:

$$\tau_3 = \frac{1}{2}\left[1 - \frac{R}{R+\Delta R} + \frac{1}{2\pi}\sin\left(\frac{2\pi R}{R+\Delta R}\right)\right]^{-1}$$

wherein R is the radius of free volume hole. ΔR is the fitted empirical electron layer thickness that equals 0.166 nm.[19]

Homo-TEOS samples cured at 110°C, 300°C, and 600°C separately have been investigated using PALS. According to the results in Table 3, free volume radius of homo-TEOS increased from 2.8 Å to 2.9 Å upon heating from 110°C to 300°C. The value further reached 3.3 Å after being cured at 600°C. The increase of free volume size with an increase of curing temperature further supports the transition from $(Si–O)_4$ to $(Si–O)_6$ ring during heating as detected by IR. Although we are not able to perform the in situ IR test above 300°C, the PALS results implies that $(Si–O)_4$ to $(Si–O)_6$ transition of homo-TEOS will take place below temperatures as high as 600°C. Within this temperature region, the higher curing temperature makes the voids of Si–O–Si chains keep growing, resulting in a looser Si–O–Si structure.

In brief, IR combined with PALS analysis suggests a reaction mechanism of:

1. Upon heating to above 80°C, there is some mobility in the oligomers. The Si–O–Si chains start to rearrange to form $(Si–O)_6$ ring before silanol condensation.

Table 3. Positron annihilation lifetime spectrum results of homo-TEOS cured at various temperatures for 1 h.

Curing temperature (°C)	110	300	600
$\tau 3$ (ns)	1.961	2.089	2.537
Mean free volume radius (Å)	2.8	2.9	3.3

2. The hydrogen-bonded silanol groups then react to form Si–O–Si linkage.
3. The previously formed $(Si–O)_4$ random network including open cage and short ladder start to be broken by further heating, through which the stressed Si–O–Si bonds of $(Si–O)_4$ ring was opened to form more continuous network with distorted $(Si–O)_6$ ring.
4. When the temperature reaches around 145°C, the residual silanol groups become isolated. There becomes to be too few hydrogen-bonded silanol groups that are possible to react, most likely directed by the diffusion. The $(Si–O)_4$ to $(Si–O)_6$ transition continues with an increase of temperature. Both of the silanol condensation and Si–O rings transition extend beyond 280°C.

TM(30–70) Silsesquioxane

A similar in situ heating IR study as described in the previous section was carried out to an organic–inorganic hybrid silsesquioxane coating. The silanol and Si–O–Si stretching IR bands of a sol-gel TM (30–70) silsesquioxane copolymer coating is shown in Figure 4. Compared with homo-TEOS, TM (30–70) SSQ exhibited similar spectral change upon heating. One apparent difference is the intensity around 1130 cm^{-1} became much stronger compared with the intensity around 1040 cm^{-1}. This result implies that the formation of symmetric cage microstructure, indicated by $(Si–O)_4$ rings, is easier in SSQ copolymer, as reported before.[2]

The PCMW results in Figure 5 and Table 4 show that the curing process of the TM (30–70) copolymer has both similarity and difference compared with that of homo-TEOS. Similar to the earlier example, during curing the spectral intensity of silanol and Si–O–Si stretching around 1100 cm^{-1} kept reducing while the Si–O–Si stretching around 1020 cm^{-1} kept increasing. The boundary of the increasing region and decreasing region of the Si–O–Si stretching band, however, shifted to a higher wavenumber region. The spectral intensity at 1040 cm^{-1} increased upon heating for TM (30–70), while in homo-TEOS it decreased. It suggests that more open $(Si–O)_6$ ring structures were formed during curing. Another difference is the higher transition temperature of TM (30–70) compared with that of homo-TEOS. The transition of homo-TEOS mainly happened at 80–145°C while the temperature shifted to 120–175°C for TM (30–70). This could be caused by the lowered silanol content in TM (30–70) compared with homo-TEOS.

Two-dimensional correlation spectroscopy analysis was also carried out and the spectra are shown in Figure 6. Silanol stretching peaks at 3348 cm^{-1} (poly-hydrogen-bonded), 3537 cm^{-1} (mono-hydrogen-bonded), 3643 cm^{-1} (SiO–H bonded to Si–O–Si), and Si–O–Si stretching peaks at 1169 cm^{-1} (closed cage of $(Si–O)_4$ ring), 1090 cm^{-1} (open cage, short ladder of $(Si–O)_4$ ring), 1030 cm^{-1}, 1014 cm^{-1}, and 999 cm^{-1} ($(Si–O)_6$ ring) were distinguished with the assignments in Table 1.[9,12,15–17] Peak intensity of $(Si–O)_6$ rings at 1030 cm^{-1}, 1014 cm^{-1}, and 999 cm^{-1} were increasing upon heating, while all the other peaks became weaker. Appearance of 1090 cm^{-1} is consistent with the original IR curves. This peak indicates that a closed cage was formed in the solution reaction for organic/inorganic hybrid SSQ material. The response sequence derived from 2D-COS is: 3348 cm^{-1} → 1030 cm^{-1} → 1169 cm^{-1} → 1014 cm^{-1} → 3537 cm^{-1} → 1090 cm^{-1} → 999 cm^{-1} → 3643 cm^{-1}. This means the condensation between poly-hydrogen-bonded silanols took place first. After that the $(Si–O)_6$ started to form with the sequence of 1030 cm^{-1} → 1014 cm^{-1} → 999 cm^{-1}, followed by the collapse of the closed cage, open cage, and ladder structure of the $(Si–O)_4$ ring. During the formation of the $(Si–O)_6$ ring, the closed cage, open cage/ladder of the $(Si–O)_4$ structure collapsed sequentially. Moreover, the mono-hydrogen-bonded silanols started to condense upon heating. At last, the isolated silanols bonded to Si–O–Si chains started to condense.

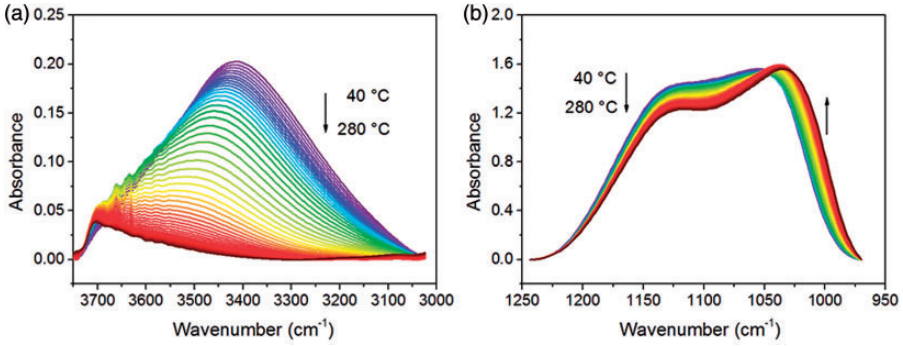

Figure 4. In situ heating IR spectra of TM (30–70) from 40°C to 280°C with 5°C of interval. (a) Infrared band of silanol stretching. (b) Infrared band of Si–O–Si stretching.

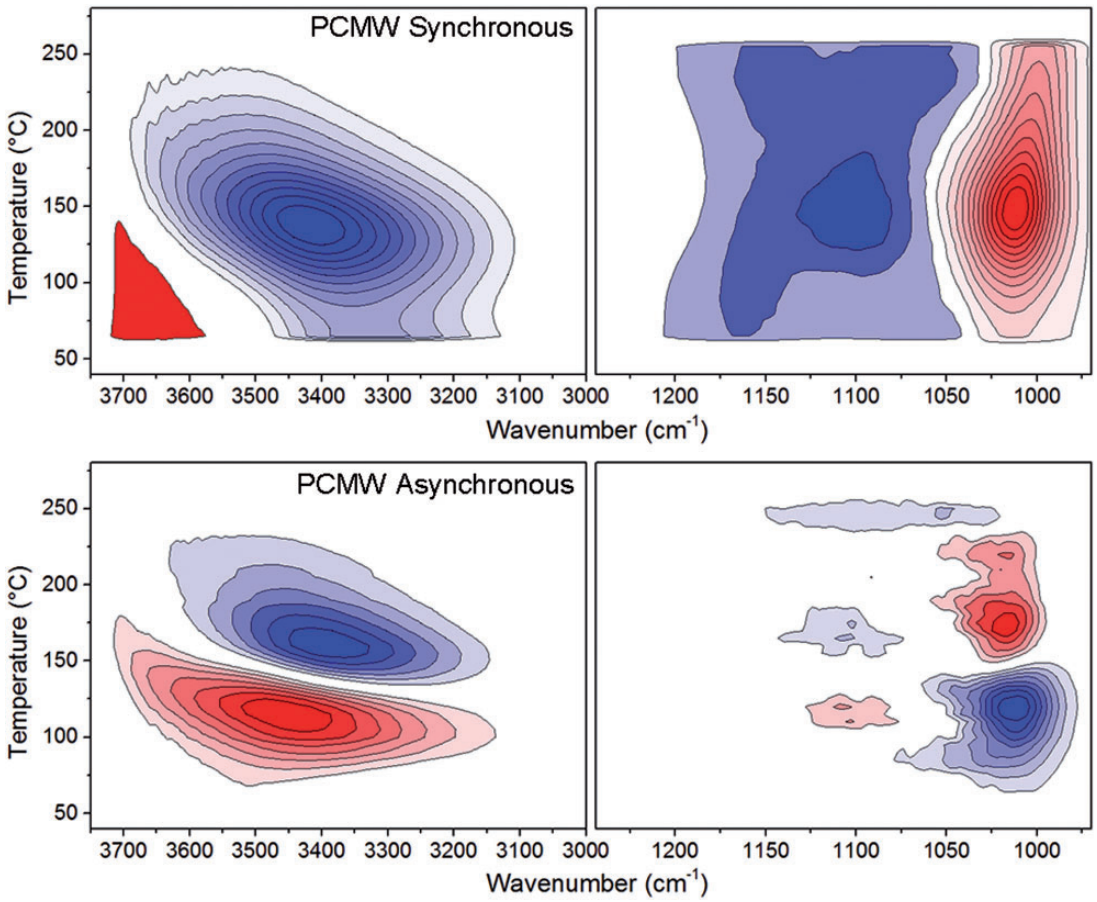

Figure 5. Perturbation correlation moving window analysis of in situ heating IR spectra of TM (30–70). (a) Synchronous spectrum; (b) asynchronous spectrum.

Table 4. Change of characteristic spectra peaks affected by curing temperature in TM (30–70) SSQ.

Changed IR bands	Direction of intensity change	Onset temperature (°C)	Peak temperature (°C)	End temperature (°C)
3500–3100 cm^{-1}, hydrogen-bonded silanol	Decrease	115	135	160
1200–1070 cm^{-1}, $(Si–O)_4$ ring in close cage	Decrease	120	150	175
1060–975 cm^{-1}, $(Si–O)_6$ ring and $(Si–O)_4$ ring in open cage and short ladder	Increase	120	150	175

Comparison of Homo-TEOS and TM (30–70)

It is meaningful to compare the behaviors of the homo-TEOS and TM (30–70) copolymer during heating. Similarly, they exhibit the same reactivity trend of silanols in various forms. The condensation starts from both poly-hydrogen-bonded silanols. After that, the mono-hydrogen-bonded silanols react. The other common thing is the transition of $(Si–O)_4$ to $(Si–O)_6$ rings. Structures with the $(Si–O)_4$ ring formed in solution tends to transform into highly cross-linked network, which is a pre-ordered structure of SiO_2 crystal.

On the other side, there are also obvious differences between the two polysiloxanes. The condensation energy barrier of homo-TESO is relatively high, because it already forms a fairly high cross-linking degree before curing. That leads to the fact that the rearrangement of the Si–O–Si chain happens ahead of condensation. This phenomenon, however, does not happen in the curing process of TM (30–70), in which silanol condensation happens first.

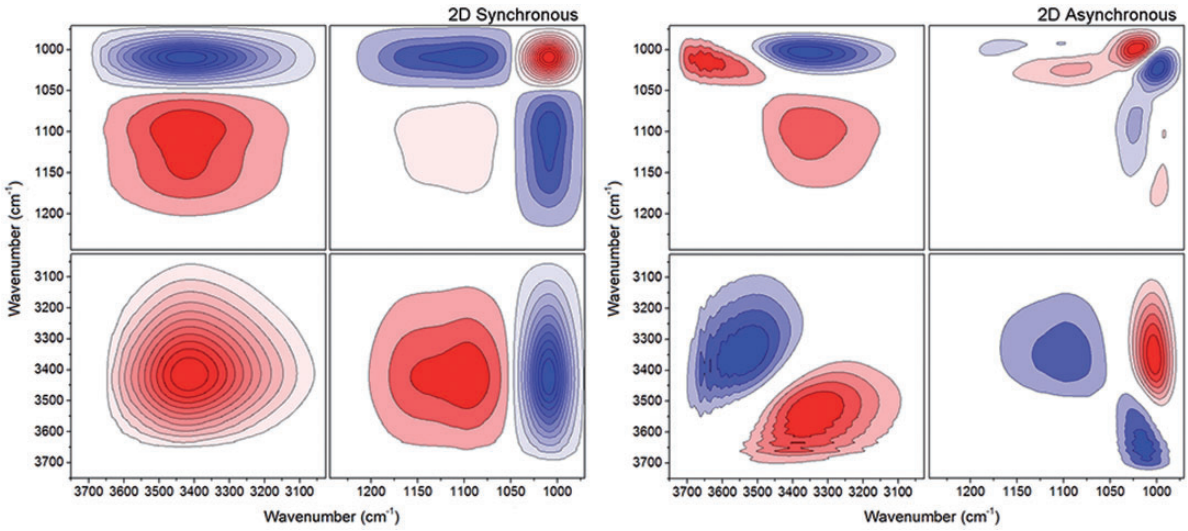

Figure 6. Two-dimensional correlation spectroscopy analysis of in situ heating IR spectra of TM (30–70) copolymer. (a) Synchronous spectrum; (b) asynchronous spectrum.

In terms of the formation of the $(Si–O)_6$ ring, only two relevant peaks are distinguished from homo-TEOS. At the end of the structural transition, the $(Si–O)_6$ structure with 1030 cm^{-1} is formed finally without any further evolution. That implies that the Si–O–Si network in homo-TEOS becomes so rigid after silanol condensation that the formed distorted $(Si–O)_6$ structure is dynamically frozen. In the case of TM (30–70), however, formation of $(Si–O)_6$ structures with 1030 cm^{-1}, 1014 cm^{-1}, and 999 cm^{-1} wavenumbers takes place sequentially, which means the structure keeps developing towards a more stable state during heating. In addition, the stability of cage and ladder structures of the $(Si–O)_4$ ring is different in these two polysiloxanes. For homo-TEOS, the peak of the closed cage cannot be distinguished. The collapse of the open cage and ladder happens ahead of the formation of a $(Si–O)_6$ ring. In the case of TM (30–70), the spectral intensity in the region from 1200 cm^{-1} to 1100 cm^{-1} become much higher and the peak of the closed cage appears at 1169 cm^{-1}. The collapse of the structures of the $(Si–O)_4$ rings takes place simultaneously with the formation of the $(Si–O)_6$ rings. Furthermore, at the end the transition, isolated silanol groups are generated in homo-TEOS. On the contrary, silanol groups with various forms in TM (30–70) continue to decrease.

The main compositional difference between these two polysiloxanes is the functionality degree of Si–O tetrahedron unit. A Si–O tetrahedron unit in homo-TESO is more reactive due to its tetra functional degree, while the organic substituents in TM (30–70) reduce the cross-linking density and plasticize the Si–O–Si skeleton. These property differences conclude that TM (30–70) exhibit higher chain flexibility compared with homo-TEOS.

Conclusions

Using the perturbation correlation moving window and 2D-COS analysis of the IR spectra, we shed new light on the curing mechanism of two siloxane materials: silica gel (homo-TEOS) and TM (30–70) silsesquioxane. The curing of polysiloxane pre-polymer involves the structural rearrangement of the Si–O–Si bonds in pre-polymers, silanol condensation, a transition of $(Si–O)_4$ to $(Si–O)_6$, and the generation of isolated silanol. For homo-TEOS, the structural evolution involves the formation of a $(Si–O)_6$ network, condensation between hydrogen-bonded silanols, collapse of the random network structures with $(Si–O)_4$ rings, and formation of a distorted $(Si–O)_6$ ring in sequence. The increase of free volume size detected by PALS is consistent with the transition of a $(Si–O)_4$ to a $(Si–O)_6$ ring detected by IR. In the case of TM (30–70), the relative reactivity of silanols in various forms was the same to that in silica gel. Transition from a $(Si–O)_4$ to a $(Si–O)_6$ ring was also observed. However, TM (30–70) exhibits a number of different properties compared with homo-TEOS. A $(Si–O)_4$ ring is more stable in TM (30–70) than in silica gel. The structural evolution started from silanol condensation rather than rearrangement of the Si–O–Si chain. In addition, silanol groups in TM (30–70) continues to decrease upon heating, while in homo-TEOS the isolated silanols were left at the end of curing. These differences could be attributed to the reduction of cross-linking caused by the organic substituents in TM (30–70), which brings higher flexibility to the Si–O–Si chain. The precise assignments of IR peaks corresponding to the Si–O–Si network needs further investigation.

Conflict of Interest

The authors report there are no conflicts of interest.

Supplemental Material

All supplemental material mentioned in the text is available at http://asp.sagepub.com/supplemental.

References

1. C.J. Brinker, G.W. Scherer. "Structural Evolution During Consolidation". In: Sol-Gel Science: The Physics and Chemistry of Sol-Gel Processing. New York: Academic, 1990. Chap. 9, pp. 518–609.
2. R.H. Baney, M. Itoh, A. Sakakibara, T. Suzuki. "Silsesquioxanes". Chem. Rev. 1995. 95(5): 1409–1430.
3. H.S. Suh, H. Kang, C.-C. Liu, P.F. Nealey, K. Char. "Orientation of Block Copolymer Resists on Interlayer Dielectrics with Tunable Surface Energy". Macromolecules. 2010. 43(1): 461–466.
4. H.W. Ro, K. Char, E.C. Jeon, H.J. Kim, D. Kwon, H.J. Lee, J.K. Lee, H.W. Rhee, C.L. Soles, D.Y. Yoon. "High-Modulus Spin-On Organosilicate Glasses for Nanoporous Applications". Adv. Mater. 2007. 19(5): 705–710.
5. W. Volksen, R.D. Miller, G. Dubois. "Low Dielectric Constant Materials". Chem. Rev. 2010. 110(1): 56–110.
6. E. Anzuresa, R. Dangelb, R. Beyelerb, A. Cannona, F. Horstb, C. Kiarie, P. Knudsena, N. Meierb, M. Moynihana, B.J. Offreinb. "Flexible Optical Interconnects Based on Silicon-Containing Polymers". Proc. SPIE. 2009. 7221: 72210I.
7. D.B. Cordes, P.D. Lickiss, F. Rataboul. "Recent Developments in the Chemistry of Cubic Polyhedral Oligosilsesquioxanes". Chem. Rev. 2010. 110(4): 2081–2173.
8. L.L. Hench, J.K. West. "The Sol-gel Process". Chem. Rev. 1990. 90: 33–72.
9. J.R. Martínez, F. Ruiz, Y.V. Vorobiev, F. Pérez-Robles, J. González-Hernández. "Infrared Spectroscopy Analysis of the Local Atomic Structure in Silica Prepared by Sol-gel". J. Chem. Phys. 1998. 109(17): 7511–7514.
10. A.J. Van Roosmalen, J.C. Mol. "An Infrared Study of the Silica Gel Surface. 1. Dry Silica Gel". J. Phys. Chem. 1978. 82(25): 2748–2751.
11. J.K. West, B.F. Zhu, Y.C. Cheng, L.L. Hench. "Quantum Chemistry of Sol-gel Silica Clusters". J. Non-Cryst. Solids. 1990. 121(1–3): 51–55.
12. E.S. Park, H.W. Ro, C.V. Nguyen, R.L. Jaffe, D.Y. Yoon. "Infrared Spectroscopy Study of Microstructures of Poly(silsesquioxane)s". Chem. Mater. 2008. 20(4): 1548–1554.
13. R.M. Almeida, T.A. Guiton, C.G. Pantano. "Characterization of Silica Gels by Infrared Reflection Spectroscopy". J. Non-Cryst. Solids. 1990. 121(1–3): 193–197.
14. R.M. Almeida, C.G. Pantano. "Structural Investigation of Silica Gel Films by Infrared Spectroscopy". J. Appl. Phys. 1990. 68: 4225.
15. T.W. Dijkstra, R. Duchateau, R.A. van Santen, A. Meetsma, G.P.A. Yap. "Silsesquioxane Models for Geminal Silica Surface Silanol Sites. A Spectroscopic Investigation of Different Types of Silanols". J. Am. Chem. Soc. 2002. 124(33): 9856–9864.
16. A. Fidalgo, L.M. Ilharco. "Correlation between Physical Properties and Structure of Silica Xerogels". J. Non-Cryst. Solids. 2004. 347(1–3): 128–137.
17. A. Fidalgo, L.M. Ilharco. "Chemical Tailoring of Porous Silica Xerogels: Local Structure by Vibrational Spectroscopy". Chem. Eur. J. 2004. 10(2): 392–398.
18. W. Brandt, S. Berko, W.W. Walker. "Positronium Decay in Molecular Substances". Phys. Rev. 1960. 120(4): 1289–1295.
19. R.A. Pethrick. "Positron Annihilation– A probe for Nanoscale Voids and Free Volume". Prog. Polym. Sci. 1997. 22: 1–47.
20. A. Shukla, M. Peter, L. Hoffmann. "Analysis of Positron Lifetime Spectra Using Quantified Maximum Entropy and a General Linear Filter". Nucl. Instrum. Methods A. 1993. 335(1–2): 310–317.
21. S. Morita, H. Shinzawa, I. Noda, Y. Ozaki. "Perturbation-correlation Moving-window Two-dimensional Correlation Spectroscopy". Appl. Spectrosc. 2006. 60(4): 398–406.
22. M. Thomas, H.H. Richardson. "Two-dimensional FT-IR Correlation Analysis of the Phase Transitions in a Liquid Crystal, 4 '-n-octyl-4-cyanobiphenyl (8CB)". Vib. Spectrosc. 2000. 24(1): 137–146.
23. I. Noda. "Two-Dimensional Infrared-Spectroscopy". J. Am. Chem. Soc. 1989. 111: 8116–8118.
24. R.M. Nieminen, M.J. Manninen. "Positrons in Imperfect Solids: Theory". In: P. Hautojärvi (ed.) Positrons in Solids. Vol 12, Berlin: Springer, 1979, pp.145–195.
25. H. Zou, S. Wu, J. Shen. "Polymer/Silica Nanocomposites: Preparation, Characterization, Properties, and Applications". Chem. Rev. 2008. 108(9): 3893–3957.